Chapter 19
$b \to s\ell\ell$ Decays at Belle

S. Choudhury, S. Sandilya, K. Trabelsi, and Anjan K. Giri

Abstract The observable R_K which is the ratio of branching fractions for $B \to K\mu\mu$ to $B \to Kee$, tests lepton flavor universality (LFU) in the standard model (SM), and hence constitutes an important probe for new physics (NP). We report herein a sensitivity study of R_K in $B \to K\ell\ell$ and of the equivalent $R_K(J/\psi)$ in $B \to KJ/\psi(\to \ell\ell)$. The latter is measured with Belle's full data sample of 772×10^6 $B\bar{B}$ pairs and the result is consistent with unity. In a variety of NP models, lepton flavor violation (LFV) comes together with LFU violation. We also report on searches for LFV in $B \to K\mu e$ and $B \to Ke\mu$ modes. Belle has recently measured LFV $B^0 \to K^{*0}\ell\ell'$ and the most stringent upper limit is found.

19.1 Introduction

The flavor changing neutral current (FCNC) decays $B \to K\mu\mu$ and $B \to Kee$ involve the $b \to s$ quark-level transition and are forbidden at tree level in the SM. These type of reactions are mediated through electroweak penguin and box diagrams, shown in Fig. 19.1. These processes are highly suppressed, have very small branching ratio ($\mathscr{B}$), and are very sensitive to NP. NP can either enhance or suppress the amplitude of the decay or may modify the angular distribution of the final state particles. The variable R_K is theoretically very clean as most of the hadronic uncertainties cancel out in the ratio. This observable is measured by LHCb [1] and the result shows a deviation of 2.6 standard deviation in the bin of $1 < q^2 < 6\,\mathrm{GeV}^2/c^4$ (q^2 = invariant-mass square of two leptons), measured for a data sample of 1 fb^{-1}. The R_K is again measured by LHCb [2] for a data sample of 3 fb^{-1} for a bin of

S. Choudhury (✉) · A. K. Giri
Indian Institute of Technology Hyderabad, Sangareddy 502285, Telangana, India
e-mail: ph16resch11007@iith.ac.in

S. Sandilya
University of Cincinnati, Cincinnati, Ohio 45221, India

K. Trabelsi
Laboratory of the Linear Accelerator (LAL), 91440 Orsay, France

P. K. Behera et al. (eds.), *XXIII DAE High Energy Physics Symposium*,
Springer Proceedings in Physics 261,
https://doi.org/10.1007/978-981-33-4408-2_19

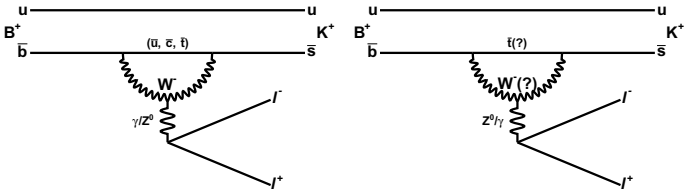

Fig. 19.1 Penguine diagram of $B \to K\ell\ell$ in SM (left) and Beyond SM (right) scenario

$1.1 < q^2 < 6\ \text{GeV}^2/c^4$ having 2.5 σ deviation. Earlier Belle [3] had also measured R_K for the whole q^2 region using a data sample of 657×10^6 $B\bar{B}$ pairs and the result was consistent with unity having very high uncertainty. The deviation from SM expectation in R_K or R_{K^*} from LHCb result may possibly show LFU violation. LFV is also an important probe to search for NP, where, LFV and LFU violation are complimentary of each other.

19.2 Monte Carlo (MC) Simulation

Our selection is based on, and optimized with an MC simulation study. One million signal events are generated using the BTOSLLBALL decay model [4] for LFU modes and phase-space for LFV modes with the EvtGen package [5]. The detector simulation is subsequently performed with GEANT3 [6].

19.3 Event Selection

We reconstruct $B \to K\ell\ell(')$ by combining a kaon (charged or neutral) with two oppositely charged leptons. Here, ℓ can be either electron or muon. The impact parameter criteria for the charged particle tracks are, along the z-axis $|dz| < 4$ cm and in the transverse plane $|dr| < 1$ cm. Charged kaon are selected based on a ratio $L_{(K/\pi)} = L_K/(L_K + L_\pi)$, where L_K and L_π are the individual likelihood of kaon and pion, respectively. For our selection, we require $L_{K/\pi} > 0.6$, which corresponds to an efficiency of above 92% with a pion fake rate below 10%. Similarly, electrons (muons) are selected with $L_e > 0.9$ ($L_\mu > 0.9$), and these correspond to an efficiency of >92% (90%) and a pion fake rate of <0.3% (<1.4%). The bremsstrahlung photon emitted by high energy electrons are recovered by considering energy deposit in a cone of 50 mrad around the initial direction of the electron track. The K^0_S candidates are reconstructed from pairs of oppositely charged tracks, both treated as pions, and are identified with a neural network (NN). The kinematic variables that distinguish signal from background are the beam-energy constrained mass

$M_{\rm bc} = \sqrt{(E_{\rm beam}/c^2)^2 - p_B^2/c^2}$ and energy difference $\Delta E = E_B - E_{\rm beam}$, where, E_B and p_B are the energy and momentum of B candidate, respectively, and $E_{\rm beam}$ is the beam energy. Events are selected within the range of $5.20 < M_{\rm bc} < 5.29$ GeV$/c^2$ and $-0.1 < \Delta E < 0.25$ GeV.

19.4 Background Rejection

The main sources of background are continuum ($e^+e^- \to q\bar{q}$) and $B\bar{B}$ events. We find that some event shape and vertex quality variables can well separate signal from background. An artificial neural network (NN) is developed using an equal number of signal and background events, where the latter is taken from continuum as well as $B\bar{B}$ samples according to their luminosity. The NN output (NN) is translated to NN' using the following transformation

$$NN' = \frac{(NN - NN_{\rm min})}{(NN_{\rm max} - NN)}$$

Here, NN_{min} is the minimum NN value, chosen to be -0.6. This criterion reduces 75% of the background with only 5–6% loss in the signal efficiency. $NN_{\rm max}$ is the maximum NN value, found from signal MC. The NN' distributions Fig. 19.2a, integrated as well as for different q^2 bins, are shown in Fig. 19.2b. It has similar shape for different q^2 regions in signal and backgrounds.

The peaking backgrounds which pass these criteria are mainly coming from $B \to J/\psi K$ because of misidentification and swapping between the leptons or lepton and kaon. These backgrounds are removed by applying invariant mass cut around J/ψ mass region. The backgrounds coming from $B^+ \to D^0(\to K^+\pi^-)\pi^+$ due to lepton

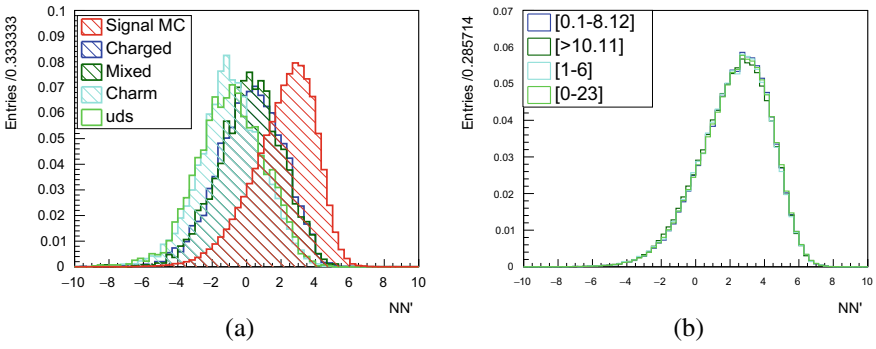

Fig. 19.2 (**a**) NN' distribution, where the red histogram represents signal MC, deep green and blue histograms are continuum and $B\bar{B}$ background, respectively. (**b**) NN' shape for different q^2 regions in signal MC events

candidates are faked by pions, and are removed by applying invariant mass cut in D^0 mass region.

19.5 Signal Yield Extraction

We perform a three-dimensional (3D) fit with $M_{\rm bc}$, ΔE, and NN'. The signal of ΔE is modeled with Crystal Ball (CB) and a gaussian function. Similarly, M_{bc} and NN' of signal are modeled with Gaussian and bifurcated gaussian-gaussian, respectively. For continuum background, the ΔE, M_{bc}, and NN' are modeled with chebychev polynomial, argus function, and Gaussian, respectively. Similarly, the $B\bar{B}$ background is fitted with exponential, argus fuction, and gaussian for ΔE, M_{bc}, and NN', respectively. From the 3D fit, the $R_K(J/\psi)$ is found to be consistent with unity and $B \to K J/\psi(\to \ell\ell)$ is used as a control sample for $B \to K\ell\ell$. The fit result for $B^+ \to K^+\mu^+\mu^-$ is shown in Fig. 19.3. The signal enhanced projections are shown in Fig. 19.4. Candidate events with $M_{\rm bc} > 5.27\,{\rm GeV}/c^2$, $|\Delta E| < 0.05$ GeV and $NN' > 0.5$ are considered to be part of the signal region.

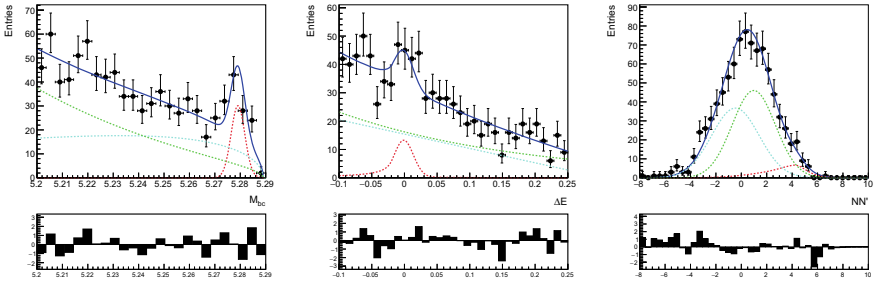

Fig. 19.3 3D fit result for a bin of $1 < q^2 < 6\,{\rm GeV}^2/c^4$ in case of $B^+ \to K^+\mu^+\mu^-$ mode. **a** $M_{\rm bc}$, **b** ΔE and **c** NN'

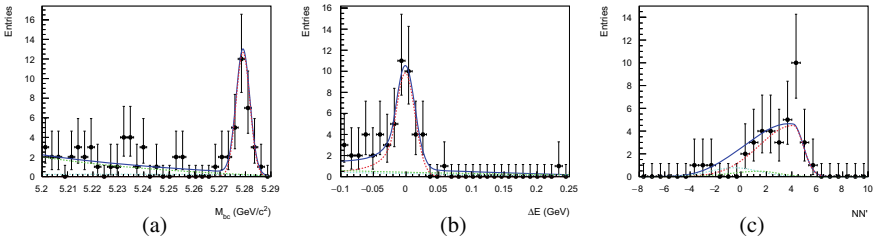

Fig. 19.4 **a** $M_{\rm bc}$ projection in the ΔE and NN' signal region **b** ΔE projection in the $M_{\rm bc}$ and NN' signal region, and **c** NN' projection in the $M_{\rm bc}$ and ΔE signal region for the bin of $1 < q^2 < 6$ ${\rm GeV}^2/c^4$ for $B^+ \to K^+\mu^+\mu^-$

19.6 Results

19.6.1 LFU Test

The statistical uncertainty of Belle for the whole q^2 region measured for a data sample of 605 fb^{-1} was 0.19 [3]. For this analysis, the expected uncertainty for the bin of $1 < q^2 < 6\ \text{GeV}^2/c^4$ is 20%, which is represented by a violet box in Fig. 19.5, here we have considered LHCb result as central value. The expected statistical uncertainty of R_K for the whole q^2 bin is 10%.

19.6.2 Search for LFV

The modes that we are studying to search LFV are $B^+ \to K^+\mu^+e^-$ and $B^+ \to K^+\mu^-e^+$. We extracted the signal from these modes by performing 3D extended maximum likelihood fit as that of LFU modes. The signal enhanced projection plots for $B^+ \to K^+\mu^+e^-$ is shown in Fig. 19.6. The upper limit is estimated from $N_{sig}^{(UL)}$, efficiency (ε) of particular mode and number of $B\bar{B}$ pairs ($N_{B\bar{B}}$), which is represented by a formula

$$\mathscr{B}^{(UL)} = \frac{N_{sig}^{(UL)}}{N_{B\bar{B}} \times \varepsilon}$$

Our estimated upper limit for LFV $B^+ \to K^+\mu^+e^-$ and $B^+ \to K^+\mu^-e^+$ are $<2.0 \times 10^{-8}$ and $<2.1 \times 10^{-8}$, respectively, as tabulated in Table 19.1, and these results are one order of magnitude better than that of the PDG values.

Belle [7] has recently searched LFV $B^0 \to K^{*0}\ell\ell'$ decays, where $\ell = \mu$ or e with full data sample. In this analysis, strong contribution from contiunnm and $B\bar{B}$

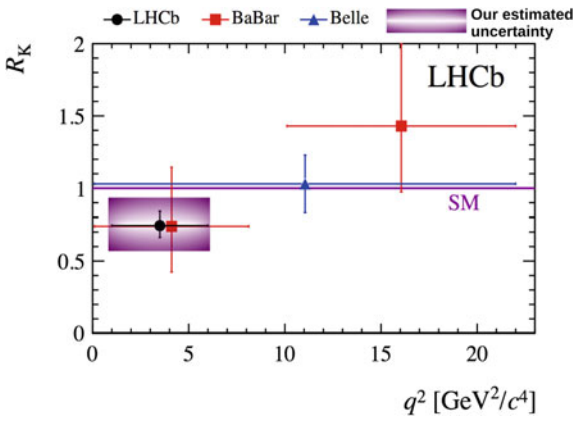

Fig. 19.5 Expected sensitivity of R_K for a bin of $1 < q^2 < 6\ \text{GeV}^2/c^4$. Here, we have considered the LHCb result as central value and the violet box represent our expected uncertainty

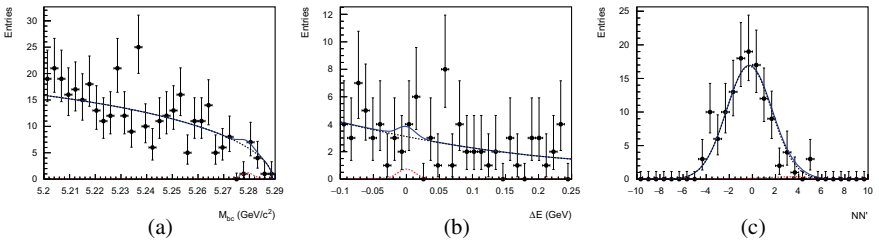

(a) (b) (c)

Fig. 19.6 Signal enhanced projection plots for $B^+ \to K^+\mu^+e^-$ mode. **a** $M_{\rm bc}$ projection in the ΔE and NN' signal region **b** ΔE projection in the $M_{\rm bc}$ and NN' signal region, and **c** NN' projection in the $M_{\rm bc}$ and ΔE signal region

Table 19.1 Upper limit estimation in MC for LFV $B \to K\ell\ell'$ modes

Mode	ε (%)	$N_{sig}^{(UL)}$	$\mathscr{B}^{(UL)}$ ($\mathbf{10^{-8}}$)	PDG $\mathscr{B}$ (10^{-7})
$B^+ \to K^+\mu^+e^-$	29.3	4.4	**2.0**	< 1.3
$B^+ \to K^+\mu^-e^+$	30.0	4.9	**2.1**	< 0.9

background is found. So, we have used two stage *NN* to suppress the backgrounds. The signal is extracted by performing extended maximum likelihood fit to M_{bc} but no evidence of signal is found and upper limit is estimated. The upper limits are $<1.2 \times 10^{-7}$, $<1.6 \times 10^{-7}$, and $<1.8 \times 10^{-7}$ for $B^0 \to K^{*0}\mu^+e^-$, $B^0 \to K^{*0}\mu^-e^+$, and $B^0 \to K^{*0}\mu^\pm e^\mp$, respectively. These observed limits are most stringent to date.

19.7 Conclusion

Several anomalies in B decays indicates lepton non-universal interaction. The LFU test is an extremely clean probe to search for NP as most of the hadronic uncertainties cancel out in the ratio of R_K. Many theoretical models predict LFV in presence of LFU violation. Belle has recently search LFV $B^0 \to K^{*0}\mu^\pm e^\mp$ and most stringent limit is found. Belle [8] will publish soon the result of R_K and LFV $B^\pm \to K^\pm\mu^\pm e^\mp$ for full data sample of 711 fb^{-1}.

Acknowledgements We thank the KEKB group for excellent operation of the accelerator; the KEK cryogenics group for efficient solenoid operations; and the KEK computer group the NII, and PNNL/EMSL for valuable computing and SINET5 network support. We acknowledge support from MEXT, JSPS and Nagoya's TLPRC (Japan); ARC (Australia); FWF (Austria); NSFC and CCEPP (China), MSMT (Czechia); CZF, DFG, EXC153, and versus (Germany); DST (India); INFN (Italy); MOE, MSIP, NRF, RSRI, FLRFAS project and GSDC of KISTI (Korea); MNiSW and NCN (Poland); MES and RFAAE (Russia); ARRS (Slovenia); IKERBASQUE and MINECO (Spain); SNSF (Switzerland); MOE and MOST (Taiwan); and DOE and NSF (USA).

References

1. R. Aaij et al., (LHCb Collaboration). JHEP **02**, 104 (2016)
2. R. Aaij et al., (LHCb Collaboration). Phys. Rev. Lett. **112**, 191801 (2019)
3. S. Wehle et al., (Belle Collaboration). Phys. Rev. Lett. **118**, 111801 (2017)
4. A. Ali, P. Ball, L.T. Handoko, G. Hiller, Phys. Rev. D **61**, 074024 (2000)
5. D.J. Lange et al., Nucl. Instrum. Meth. **A462**, 152 (2001)
6. R. Brun et al., CERN Report No. **DD/EE**, 84-1 (1984)
7. S. Sandilya et al., (Belle Collaboration). Phys. Rev. D **98**, 071101 (2018)
8. S. Choudhury et al., (Belle Collaboration), arXiv:1908.01848